

UNCLASSIFIED

AD 266 787

*Reproduced
by the*

ARMED SERVICES TECHNICAL INFORMATION AGENCY
ARLINGTON HALL STATION
ARLINGTON 12, VIRGINIA



UNCLASSIFIED

NOTICE: When government or other drawings, specifications or other data are used for any purpose other than in connection with a definitely related government procurement operation, the U. S. Government thereby incurs no responsibility, nor any obligation whatsoever; and the fact that the Government may have formulated, furnished, or in any way supplied the said drawings, specifications, or other data is not to be regarded by implication or otherwise as in any manner licensing the holder or any other person or corporation, or conveying any rights or permission to manufacture, use or sell any patented invention that may in any way be related thereto.

CATALOGED BY ASTIA
AS AD NO. 266787

HE-150-190
TECHNICAL REPORT

UNIVERSITY OF CALIFORNIA
INSTITUTE OF ENGINEERING RESEARCH
BERKELEY, CALIFORNIA



NOX
62-1-3

EXPERIMENTAL DETERMINATION OF PITCHING MOMENT AND DAMPING COEFFICIENTS
OF A CONE IN LOW DENSITY, HYPERSONIC FLOW

By

Walter Leo Maas

SERIES NO. 20
ISSUE NO. 135
DATE October 9, 1961

CONTRACT N-onr-222(45)
REPORT NO. HE-150-190
SERIES NO. 20-135
OCTOBER 9, 1961

JOINTLY SPONSORED BY
THE OFFICE OF NAVAL RESEARCH AND
THE OFFICE OF SCIENTIFIC RESEARCH

EXPERIMENTAL DETERMINATION OF PITCHING MOMENT AND DAMPING COEFFICIENTS
OF A CONE IN LOW DENSITY, HYPERSONIC FLOW

By

Walter Leo Maas


A portion of a Masters Thesis in Mechanical Engineering

Reproduction in whole or in part is permitted for
any purpose of the United States Government

FACULTY INVESTIGATORS:

S. A. SCHAAF, PROFESSOR OF ENGINEERING SCIENCES
G. J. MASLACH, PROFESSOR OF AERONAUTICAL ENGINEERING
L. TALBOT, ASSOCIATE PROFESSOR OF AERONAUTICAL SCIENCES

Approved



ABSTRACT

Values of the stability derivatives $C_{m\alpha}$ and C_{mq} have been determined experimentally for cones with semi-vertex angles of 45° and 9° , and the results compared with theoretical estimates and with other experimental data. $C_{m\alpha}$ is seen to be a function of angle of attack, and C_{mq} is found to be positive, indicating negative damping. The influence of viscous effects upon these results is discussed.

The experiment was conducted with freely oscillating models in hypersonic, low density flow, and is one of the first dynamic stability tests performed under these flow conditions. $C_{m\alpha}$ deviates sharply from linear theory, the non-linearity being even stronger than predicted by current non-linear Newtonian flow theory.

C_{mq} was found to be positive in sign, meaning negative damping and an input of energy to the model from the flow. This instability is a marked deviation from the ordinary assumption of positive stability and certainly warrants further study and investigation. The cause of the instability remains undetermined; the effects of viscous flow and shedding of vortices is discussed in this connection.

TABLE OF CONTENTS

	<u>Page</u>
ABSTRACT	i
LIST OF SYMBOLS	iv
1. INTRODUCTION	1
1.1 Theoretical Basis	1
1.2 Induced Oscillation Technique	2
1.3 Free Oscillation Technique	3
2. PRELIMINARY CONSIDERATIONS	4
2.1 Induced Oscillation Technique	5
2.2 Free Oscillation Technique	6
3. EXPERIMENTAL EQUIPMENT	7
4. EXPERIMENTAL PROCEDURE AND DATA REDUCTION	8
4.1 $C_{m\alpha}$	8
4.2 C_{mq}	8
4.3 Other Parameters	9
5. RESULTS	9
6. EXPERIMENTAL ACCURACY	10
6.1 $\bar{C}_{m\alpha}$	10
6.2 \bar{C}_{mq}	10
7. DISCUSSION OF RESULTS	11
7.1 $\bar{C}_{m\alpha}$	11
7.2 \bar{C}_{mq}	14
REFERENCES	18
APPENDIX A - Determination of \bar{C}_{mq}	19
APPENDIX B - Moment of Inertia Determination	21

	<u>Page</u>
APPENDIX C - Error Analysis	22
FIGURES	23
1. Fixture Mounted on Nozzle with 45° Cone	23
2. Fixture with 9° Cone	24
3. Values of $\bar{C}_{m\alpha}$ for Various Oscillation Angles (α_o). 45° & 9° Semi-Vertex Angle Cones.	25
4. $\bar{C}_{m\alpha}$ & $C_{m\alpha}$ as a Function of Oscillation Angle	26
5. $C_{N\alpha}$ vs α Newtonian Flow Solution	27
6. Oscillation Frequency vs Angle	28
7. Plot of \bar{C}_{mq} vs Oscillation Angle	29

LIST OF SYMBOLS

(Other Symbols are defined as used)

b	coefficient of damping term = $\frac{\rho U S L^2}{2I} (-C_{mq})$
C_m	standard non-dimensionalized moment coefficient
$C_{m\alpha}$	restoring moment derivative
C_{mq}	damping derivative
$\bar{C}_{m\alpha}, \bar{C}_{mq}$	average values. See Section 5
D	rate of decay of oscillation ($^\circ/\text{sec}$)
I	mass moment of inertia about axis of oscillation
k	coefficient of restoring moment term = $\frac{\rho U^2 S L}{2I} (-C_{m\alpha})$
L	reference length = axial length of cone
M	Mach number
Re/in	Reynolds number per inch = $\frac{u\rho}{\nu}$
S	reference area = base area of cone
t	time
T	period of oscillation = $\frac{2\pi}{\omega'}$
u, w	linear flow velocity components parallel to and perpendicular to axis of revolution, respectively

U	velocity of undisturbed airflow
X	distance from nose of cone to center of oscillation
α	angle of attack
α_o	oscillation angle or envelope of angle of attack
γ	cone semi-vertex or half angle
ρ	mass density of atmosphere
ϕ	phase angle
θ	angle of rotation
ω	angular velocity or frequency $\left(\frac{\text{radians}}{\text{sec}} \right) \quad \omega = \frac{2\pi}{T}$

1. INTRODUCTION

The motion of an oscillating cone is described by the well-known second order differential equation containing inertia, damping and restoring moment terms. These terms can be evaluated experimentally by study of the motion in a wind tunnel airstream. This report covers such a test in low density, hypersonic flow; it is in the nature of a feasibility study since there is little background of dynamic stability tests under such conditions.

1.1 Theoretical Basis

The linearized equation of motion of natural short period longitudinal oscillations is given by Laitone¹ as

$$I\ddot{\theta} + \left(\frac{\rho u S L}{2} \frac{\partial c_m}{\partial \alpha} \right) w + \left(\frac{\rho u S L^2}{2} \frac{\partial c_m}{\partial \left(\frac{\dot{\theta} L}{u} \right)} \right) \dot{\theta} + \left(\frac{\rho S L^2}{2} \frac{\partial c_m}{\partial \left(\frac{\dot{\alpha} L}{u} \right)} \right) \dot{w} = 0 \quad (1)$$

It can be shown that $\partial c_m / \partial \left(\frac{\dot{\alpha} L}{u} \right)$ is negligible in hypersonic, low density flow, leaving

$$I\ddot{\theta} + \left(\frac{\rho u S L}{2} c_{m\alpha} \right) w + \left(\frac{\rho u S L^2}{2} c_{mq} \right) \dot{\theta} = 0 \quad (2)$$

where $c_{m\alpha} = \frac{\partial c_m}{\partial \alpha}$

$$c_{mq} = \frac{\partial c_m}{\partial \left(\frac{\dot{\theta} L}{u} \right)}$$

as $\alpha \rightarrow 0$
 $\dot{\theta} \rightarrow 0$
 $\dot{\alpha} \rightarrow 0$

This is an ordinary second order linear differential equation, with the linearization implying small values of θ .

1.2 Induced Oscillation Technique

It was first proposed (by Professor E. V. Laitone of the University of California) that the stability coefficients of a cone be evaluated by an induced oscillation technique in the wind tunnel. The cone model would be fixed on a shaft (sting) passing through and perpendicular to the axis of revolution of the cone. This sting would be mounted in bearings and the model, with sting, would be free to revolve in these bearings. However, the bearing supports, and therefore the model, would be oscillated in a plane perpendicular to the flow, with a velocity

$$\dot{z}(t) = a\omega \sin \omega t \quad (3)$$

where a = amplitude of oscillation
 z = linear displacement of sting
 ω = frequency of oscillation

Then in a wind tunnel of velocity $U = u$

$$\frac{w}{U} = \left(\theta + \frac{\dot{z}}{U} \right) = \theta + \frac{a\omega}{U} \sin \omega t \quad (4)$$

and Equation (2) becomes

$$\ddot{\theta} + b\dot{\theta} + k\theta = -k \frac{a\omega}{U} \sin \omega t \quad (5)$$

$$\text{where } b = \frac{\rho U S L^2}{2I} \left(-C_{m_q} \right)$$

$$k = \frac{\rho U^2 S L}{2I} \left(- C_{m\alpha} \right)$$

By measuring the amplitude $(\dot{\theta})$ and phase angle $(\varphi_{\dot{\theta}})$ of the angular velocity $\dot{\theta}$ at different frequencies ω , C_{mq} and $C_{m\alpha}$ can be determined by a circle or Nyquist plot (see reference 2), where

$$\left. \begin{aligned} \text{vector length} &= \frac{|\dot{\theta}|}{\omega a/L} = - \frac{C_{m\alpha}}{C_{mq}} \cos \varphi_{\dot{\theta}}(\omega) = \frac{|\theta|}{a/L} \\ \text{vector angle} &= \varphi_{\dot{\theta}}(\omega) \\ &= \tan^{-1} \left[\frac{U}{\omega L} \frac{C_{m\alpha}}{C_{mq}} - 2 \frac{I/\rho S L^3}{\omega L (-C_{mq})} \right] \\ &= \varphi_{\theta}(\omega) + \frac{\pi}{2} \end{aligned} \right\} (6)$$

Therefore, in principle, the aerodynamic derivatives $C_{m\alpha}$ and C_{mq} can be found. However, it will be shown in Section 2.1 that this method is not feasible in hypersonic flow, and it is necessary to turn elsewhere for an acceptable technique.

1.3 Free Oscillation Technique

In this method the model is free to oscillate in the sting bearings as before, however the bearings remain stationary. The motion of the model is purely oscillation about a fixed axis, under the influence of bearing friction and aerodynamic forces. Here

$$\theta = \frac{w}{U} = \alpha, \quad \dot{\theta} = \dot{\alpha}, \quad \ddot{\theta} = \ddot{\alpha} \quad (7)$$

and Equation (2) becomes

$$\ddot{\alpha} + b\dot{\alpha} + k\alpha = 0 \quad (8)$$

Adding an arbitrary bearing friction torque $f(\dot{\alpha})$ gives the equation of motion of the system

$$\ddot{\alpha} + b\dot{\alpha} + f(\dot{\alpha}) + k\alpha = 0 \quad (9)$$

With small damping, the frequency of oscillation is

$$\omega = \sqrt{k} = \sqrt{\frac{\rho U^2}{2} \frac{SL}{I} (-C_{m\alpha})} \quad (10)$$

$$\text{or } C_m = -\omega \frac{2}{\rho U^2} \frac{I}{SL} = -\left(\frac{2\pi}{T}\right)^2 \frac{2}{\rho U^2} \frac{I}{SL}$$

$C_{m\alpha}$ can be simply found by a measurement of the period of oscillation of the model, and determination of the model parameters I , S and L and the dynamic pressure $\frac{\rho U^2}{2}$.

The derivative C_{mq} is a measure of the aerodynamic damping present. This damping in turn can be found by observing the rate of decay of the oscillation amplitude as the model is given an initial displacement and allowed to oscillate in the flow stream.

2. PRELIMINARY CONSIDERATIONS

From the beginning of this program it was apparent that the aerodynamic damping would be small compared to the restoring moment. Since

$$\frac{b}{k} = \frac{C_{m_q}}{C_{m_\alpha}} \frac{L}{U} \quad (11)$$

and using estimated values

$$\begin{aligned} C_{m_\alpha} &= -4/3 & L &= 0.625 \text{ in} \\ C_{m_q} &= -2 & U &= 2370 \text{ ft/sec} \end{aligned}$$

then $b/k = 10^{-4}/3$, an extremely small amount of damping. The factor L/U shows the difficulty; in hypersonic flow and with the model size restriction imposed by the flow nozzle, L/U becomes very small.

2.1 Induced Oscillation Technique

Equation (6) can be written

$$\begin{aligned} \phi_\theta(\omega) &= \tan^{-1} \frac{\frac{k}{\omega} - \omega}{b} \\ &= \tan^{-1} \frac{\omega_o^2 - \omega^2}{\omega b} \end{aligned} \quad (12)$$

where ω_o = natural or undamped
oscillatory frequency

$$= \sqrt{k}$$

Since b is small, ω will be very close to ω_o and any slight fluctuation in this difference will have a strong effect upon the vector position.

A preliminary calculation, using typical $M = 6$ low density flow values and a 45° semi-vertex angle cone model with $L = 0.625$ in,

showed that a frequency $\omega = 1.0015 \omega_0$ would shift the phase vector to $\phi = 45^\circ$, and $\omega = 1.0060 \omega_0$ corresponds to $\phi = 84.3^\circ$. Tunnel flow characteristics are such that ρU^2 fluctuates as much as $\pm 2\%$, and since $\omega_0 \sim \sqrt{\rho U^2}$, ω_0 would vary $\pm 1\%$. Such a natural frequency variation would cause almost a 180° oscillation in the phase vector, rendering it useless in determining the aerodynamic coefficients and derivatives.

Essentially, the small amount of damping forces the induced frequency (ω) to be very close to the natural frequency (ω_0) in order to use the Nyquist plot, and with the flow irregularities inherent in the wind tunnel, ω_0 fluctuates enough to make $\phi = \tan^{-1} (\omega_0^2 - \omega^2) / \omega b$ completely undefinable. This conclusion resulted in abandonment of the induced oscillation technique.

2.2 Free Oscillation Technique

Determination of $C_{m\alpha}$ by observing the period of oscillation presented no serious problems, however the low aerodynamic damping again gave difficulty in finding C_{mq} . The amplitude decay caused by bearing friction would be relatively large and could easily obscure the aerodynamic damping. Information on low-friction bearings gave a minimum of 7 dyne-cm of resistance torque for the proposed system. Using this figure, calculations at $M = 6$ flow conditions showed that the damping from the bearings would be approximately 10 times the aerodynamic damping.

On the basis of this information, it was decided to use the free oscillation technique to determine $C_{m\alpha}$, with the possibility that C_{mq} could also be found. C_{mq} would be a function of the difference in decay rate between the model oscillating in the airflow and oscillating in the evacuated tunnel without flow. This relationship is described in detail in Appendix A.

3. EXPERIMENTAL EQUIPMENT

The tests were conducted in the No. 4 low density wind tunnel at the University of California Aeronautical Sciences Laboratory, Richmond Field Station. The Mach 6 nozzle was used, providing a test section approximately 2.5 inches in diameter. The fixture holding the model was mounted directly on the end of the nozzle, as shown in Figure 1.

Figure 2 shows the 9° cone model mounted on the fixture. The model is fixed on the vertical sting, the sting being supported by two electrically vibrated bearings. A cross shaft is mounted on the sting above the upper bearing. One arm of this shaft carries a blade which interrupts the light beam to a photocell as the model passes through zero angle of attack. The other arm is attracted by an electromagnet mounted on the tunnel, thereby pulling the model to an angle of attack. Release of the arm starts the oscillation. In addition, a shadow cast by this arm is projected upon a calibrated screen, providing direct oscillation angle (α_0) information.

As shown in Figure 1, a cardboard and plastic cover shields the arm from extraneous air currents. The quartz fiber is shown suspended from above and attaches to the tip of the sting. The sting itself (here carrying the 45° cone) has a tungsten carbide center section 2 inches long and 0.078 inches in diameter. This design represents a compromise between sting structural stiffness and minimum aerodynamic interference, several configurations were tried with this being the most satisfactory.

The photocell output is fed to an electronic counter which times the interval between pulses and presents this time on a visual readout. Since the swinging arm interrupts the photocell beam twice

complete oscillation, the time shown is one half the period of oscillation.

The bearings have an electrically vibrated inner bearing race, which reduces friction torque to a minimum by eliminating static friction. They are the most suitable bearings that could be found for this application, although devices such as air and magnetic suspension may have even less friction. These possibilities were not explored.

4. EXPERIMENTAL PROCEDURE AND DATA REDUCTION

4.1 $C_{m\alpha}$

The model was given an initial displacement of approximately 35° and allowed to oscillate in the flow stream. Oscillation period data from the electronic counter was recorded at $\alpha_o = 30^\circ, 20^\circ, 15^\circ, 10^\circ, 5^\circ$, and 3° . This period gave $C_{m\alpha}(\alpha_o)$ directly through the relationship

$$C_{M\alpha} = - \left(\frac{2\pi}{T} \right)^2 \frac{2I}{\rho U^2 SL}$$

4.2 C_{Mq}

A stopwatch was used to determine the oscillation decay rate. As the motion decayed through values of $\alpha_o = 30^\circ, 20^\circ, 15^\circ, 10^\circ$, and 5° , the time was recorded. The average decay rate was computed in the intervals between these values by dividing the particular interval (in degrees) by the time the model took to decay through this interval. This value was taken as the decay rate at the angle in the mid-point of the interval. For example, in the interval between 15° and 10° , the decay

rate would be the interval (5°) divided by the decay time (in seconds) from 15° to 10° . This value is then the decay rate existing at $\alpha_o = 12.5^\circ$.

As described in Appendix A, this decay test is performed under both no flow and flow conditions, the difference in rate of decay giving the value of C_{mq} . Using this method, C_{mq} can be found for $\alpha_o = 25^\circ$, 17.5° , 12.5° , and 7.5° .

4.3 Other Parameters

The moment of inertia of the system (I) was computed as described in Appendix B. S and L were accurately measured using ordinary machine shop techniques. Flow information (ρ , M, U, and Re/in) were computed from compressible flow charts using flow pressure and temperature data recorded with each run.

5. RESULTS

Two cone models were tested, one having a semi-vertex angle $\gamma = 45^\circ$, and the other $\gamma = 9^\circ$. For the 45° cone, $X/L = 0.337$, for the 9° cone, $X/L = 0.350$. The average flow conditions in these tests were $M = 6.05$, $Re/in = 11,700$, $U = 2375$ ft/sec, $\frac{\rho U^2}{2} = 0.0530$ psi, and a static pressure of 125 microns of mercury.

Values of $C_{m\alpha}$ are tabulated in Figure 3 and shown in graphical form in Figure 4. C_{mq} is plotted in Figure 7. These values are given as functions of α_o , the angle of oscillation. No attempt has been made to define them as functions of the instantaneous angle of attack, (α), and since both $C_{m\alpha}$ and C_{mq} vary with angle of attack, the figures given represent an average or effective value over a single

oscillation. Hereafter these effective values will be designated as $\bar{C}_{m\alpha}$ and \bar{C}_{mq} .

6. EXPERIMENTAL ACCURACY

A numerical error analysis is given in Appendix C; the figures below are derived therein.

6.1 $\bar{C}_{m\alpha}$

The uncertainty in the values of $\bar{C}_{m\alpha}$ is between 3.0% and 3.6%, depending upon α_o . The prime contributors to this inaccuracy are U , T , and α_o . The error in U is inherent in the flow stream and cannot be improved with the present tunnel and nozzle. The uncertainty in T is based upon data scatter; refinement of technique could possibly lower this somewhat. The inaccuracy in α_o is discussed fully in the next section. These values of $\bar{C}_{m\alpha}$ are about as precise as presently possible; it would be difficult to better them significantly without improving U .

6.2 \bar{C}_{mq}

The small magnitude of damping and the relatively crude decay rate measurements lead to the large uncertainties in \bar{C}_{mq} . It is felt that a more sophisticated experimental system is necessary to derive accurate data.

The difficulties arise with the measurement of α_o and with the bearing friction. The present method of reading α_o (shadow of swinging arm projected on a calibrated screen) causes the 29% uncertainty in decay rate data; an improved system here would definitely improve the measured value of \bar{C}_{mq} .

Aerodynamic damping is small compared to damping from bearing friction, consequently in the subtraction of decay rates (see Appendix A) two nearly equal numbers with moderate uncertainties are subtracted, the difference being small in magnitude and having a large uncertainty.

A solution here would be to reduce bearing friction. The bearings used are claimed to be the best conventional bearings available, however devices such as air suspension and suspension by fibers would warrant investigation for further experiments.

7. DISCUSSION OF RESULTS

7.1 $\bar{C}_{m\alpha}$

Figure 4 presents the experimentally derived values and compares them with other data, both theoretical and experimental.

On the ordinate $\alpha_0 = 0$ the small angle values of $C_{m\alpha}$ from the theory of Coakley, Laitone, and Maas³ and also from Tobak and Wehrend⁴ are plotted. They are seen to be in reasonable agreement with the experimental values, the 45° cone particularly. Both theoretical analyses require $\alpha < \gamma$ (all elements of the cone must "see" or face the flow), the 9° cone is near this limit even at small α_0 , which might explain the great deviation.

The bottom curve is from the experimental data of Maslach and Talbot⁵ (obtained under the same flow conditions as this report) on the static moment of a 9° cone. From their plot of C_m vs α (corrected for center of oscillation position) the slope of the secant line between $\alpha = 0$ and $\alpha = \alpha_0$ was taken as the average slope of $C_{m\alpha}$ during an oscillation bounded by α_0 . Therefore the values plotted are $\bar{C}_{m\alpha}$ and

are directly comparable to the experimental values. It is seen that $\bar{C}_{m\alpha}$ from the static test is generally smaller than that from the dynamic test and varies less with angle of attack. These differences are probably caused by unsteady flow effects around the oscillating cone and are seen to be appreciable in this hypersonic, low density flow regime.

Charwat⁶ develops a Newtonian flow analysis for the normal force derivative $C_{N\alpha}$ (which is proportional to $C_{m\alpha}$ assuming a stationary center of pressure) for $\alpha < \gamma$ and also for the case where half of the surface of the body sees the flow. For a cone this latter solution is strictly valid for $\alpha = 90^\circ$ only, but the extension of this theory to lower angles of attack can give an indication of the variance of $C_{m\alpha}$ with α (or α_0) for the 9° cone.

The two solutions of Charwat are shown in Figure 5, with a curve (dashed line) faired between the two being more representative of the actual case. It is seen that $C_{N\alpha}$ (and therefore $C_{m\alpha}$) generally increases with angle of attack up to $\alpha = 35^\circ$. This correlates well with the experimental values of $C_{m\alpha}$ for the 9° cone shown in Figure 4, where $\bar{C}_{m\alpha}$ is seen to increase with α_0 .

Coakley, et. al., also give a hypersonic, Newtonian flow motion analysis not restricted to small angles of attack, requiring only that $\alpha < \gamma$. Their non-linear equation of motion is (disregarding damping):

$$\alpha + \frac{\rho U^2}{2I} SL \left[4/3 - 2 \frac{X}{L} \cos^2 \gamma \right] \frac{\sin 2\alpha}{2} = 0 \quad (13)$$

Using the expansion $\frac{1}{2} \sin 2\alpha = \alpha - \frac{2}{3} \alpha^3 + \dots$ the frequency of oscillation of motions governed by this equation is

$$\omega = 2\pi \sqrt{\frac{\rho U^2}{2} \cdot \frac{SL}{I} \left[\frac{4}{3} - 2 \frac{X}{L} \cos^2 \gamma \right]} \sqrt{1 - \frac{1}{2} \alpha_0^2} \quad (14)$$

Figure 6 compares this relationship ρ , U , S , L and I taken the same as in experiment) with the frequencies obtained in the 45° cone experiment. It is seen that the decrease in ω with larger α_0 is even stronger than predicted by the non-linear theory.

Apparently, these differences are caused by viscous effects. Newtonian flow theory, of course, does not consider the boundary layer and wake phenomena which certainly influence the motion, especially at large α . Very little is known about hypersonic viscosity effects upon dynamic stability; the experimental results here indicate that they are appreciable and should be further investigated.

It should be noted that all the values of $\bar{C}_{m\alpha}$ are negative, indicating positive static stability in equations (8) and (9). For the case of a missile returning to earth through the atmosphere, Allen⁷ shows that it is only necessary that $C_{m\alpha} < 0$ for static stability, after considering the effects of the earth's gravitational field, deceleration due to aerodynamic drag and variance of atmospheric density with the altitude. Thus, it seems that static stability of a conical missile is assured as long as the center of gravity (and therefore the axis of oscillation) is well forward, as in these tests. As Allen points out, however, static instability can occur with a c.g. position towards the rear of the missile.

It is felt that the values of $\bar{C}_{m\alpha}$ found in these experiments are representative of the models tested. It is not possible to improve the experimental accuracy significantly without improving the flow

characteristics of the wind tunnel. However, it does seem that tests with the center of oscillation moved aft would be worthwhile, since a point would be reached where $C_{m\alpha} > 0$ and the cone is statically unstable. For small α this point would be near the center of pressure, but for larger oscillations (as in these tests) the point of instability cannot be predicted theoretically, and a wind tunnel test is called for.

7.2 \bar{C}_{mq}

The values of \bar{C}_{mq} shown in Figure 7 have such a high experimental uncertainty that they must be considered in a qualitative sense only. Very little can be said of their absolute magnitude, except that perhaps \bar{C}_{mq} for the 45° cone decreases with α_o and for the 9° cone increases with α_o .

It should be realized that \bar{C}_{mq} has been found to be positive, indicating negative damping and dynamic instability. In every test on both cones, the model took longer to decay (from 30° to 5°) when under flow than it did with no flow. This is indicative of energy input into the model from the airflow.

This instability here only partially counteracts the bearing friction damping, and the oscillations still decrease. However, in an object in free flight, instability would tend to cause increasing oscillations (disregarding the influence of other damping factors, of course). For this reason it is apparent that the instability found here is important and should be investigated further.

All the available theory predicts $C_{mq} < 0$, and previous experiments (at lower Mach numbers) show $C_{mq} < 0$ and nearly independent

of the angle of attack. It must be emphasized, though, that hypersonic Newtonian flow theory does not consider any variation in the pressures on the rear of a cone, and this effect could be important for a cone oscillating in a flow stream. An analytical study, one including viscous effects and not restricted to small α , would certainly be difficult, but might reveal the nature of this instability.

There seem to be no prior dynamic stability experiments of this type in hypersonic flow. Further investigation is certainly in order, both to more accurately determine C_{mq} , and especially to investigate the nature of the instability.

As stated earlier, the large uncertainty in \bar{C}_{mq} stems from the small amount of damping present. With the model size restriction of the flow nozzle, the ratio b/k will be small in hypersonic flow unless \bar{C}_{mq} (and therefore k) is reduced by oscillating the model on an axis near the center of pressure. Unfortunately, reducing the restoring moment in this manner increases the adverse effect of bearing friction, so this method most likely would not be an improvement.

Perhaps a free flight 'shot' in a ballistic-type tunnel would be the solution--here there would be no bearing friction and the model would oscillate about its center of mass. High speed photographs could provide an oscillation-time history; the decay (or increase) in the oscillation would give the damping. However, deceleration from aerodynamic drag introduces other terms into the damping coefficient; these might prove difficult to separate from \bar{C}_{mq} .

More accurate determination of \bar{C}_{mq} would be possible by improvement of the present apparatus. The uncertainty in α_0 ($\pm 1^\circ$) is large and certainly could be decreased. An improved optical system or high speed motion pictures might be the solution.

Decreasing the bearing friction would increase the relative effect of the aerodynamic damping and thereby improve the accuracy of \bar{C}_{mq} . The bearings used here are probably as friction free as possible in a mechanical system, but perhaps could be improved slightly. Magnetic or air suspension might be feasible, although it would be difficult to avoid the air or magnetic field affecting the motion of the model.

Suspension by a quartz fiber has definite possibilities, for quartz has very little internal friction and a quartz torsional pendulum decays very slowly. A model made from a heavy material such as lead could be hung in the airflow from a quartz fiber, perhaps with another fiber holding it from below.

Reducing the friction of the suspension device and decreasing the uncertainty in α_0 would permit an accurate plot of α_0 vs time. The slope of this curve could easily be found by use of a least squares program on a digital computer. This would eliminate the averaging method used in this report and provide accurate values of decay rate at any α_0 .

Another avenue for further investigation is the cause of the negative damping. As previously mentioned, there has been no prior indication of dynamic instability from either theoretical or experimental studies, although little work has been done in either field on oscillating bodies in hypersonic flow.

Possibly the instability is due to the asymmetrical shedding of vortices from the sharp trailing edge of the cone. Very little is understood about vortex formation on three-dimensional oscillating bodies, but it is possible to make a few statements concerning their effect.

It is known that vortices depart in a periodic manner from stationary bodies of revolution at zero angle of attack, and that they affect the pressure distribution on the surface of the body. It seems reasonable, then, that pressures on an oscillating body are also affected by vortex formation. If these pressure fluctuations occur in a manner so as to transfer energy from the flow to the model (i.e., the additional torque from the pressure fluctuation acts in the same direction as the rotational velocity, rather than being a torque opposing the velocity as in ordinary positive damping) there is negative damping. This might well be what is happening here.

The vibration of electric power lines in a crosswind is well-known; this is an example of aerodynamic instability from vortex formation on a two-dimensional body. Goldstein⁸ speaks of the oscillatory nature of vortex departure behind a flat circular disc and also of vortex instability behind a two-dimensional cylinder. Unfortunately, none of the information available specifically pertains to an oscillating, three-dimensional body.

As a feasibility study, this program was successful first in that the induced oscillation technique was shown to be impractical, and also that $\bar{C}_{m\alpha}$ could be easily determined by the free oscillation technique. \bar{C}_{mq} was found to a rather poor degree of uncertainty, but improvement of the experimental apparatus could produce more accurate results.

REFERENCES

1. Laitone, E. V., "Effect of Acceleration on the Longitudinal Dynamic Stability of a Missile," ARS Journal, 29, 2, February 1959.
2. Milliken, W.F., Jr., "Progress in Dynamic Stability and Control Research," J. Aero. Sci., 14, 9, 493, September 1947.
3. Coakley, T.J., Laitone, E.V., & Maas, W.L., "Fundamental Analysis of Various Dynamic Stability Problems for Missiles," Univ. of Calif., Inst. of Eng. Res. Report, Series No. 176-1, June 1961.
4. Toback, M., & Wehrend, W.R., "Stability Derivatives of Cones at Supersonic Speeds," NACA TN-3788, September 1956.
5. Maslach, G.J., & Talbot, L., "Low Density Aerodynamic Characteristics of a Cone at Angle of Attack," Univ. of Calif. Eng. Project Report HE-150-172, October 1959.
6. Charwat, A.F., "The Stability of Bodies of Revolution at Very High Mach Numbers," Jet Propulsion, 27, 8, August 1957.
7. Allen, H. Julian, "Motion of a Ballistic Missile Angularly Misaligned with the Flight Path Upon Entering the Atmosphere and its Effect upon Aerodynamic Heating, Aerodynamic Loads, and Miss Distance," NACA TN-4048, October 1957.
8. Goldstein, S. (Editor), "Modern Developments in Fluid Dynamics," Vol. 2, Oxford Press, London, 1938, pp 570-592.

APPENDIX A

DETERMINATION OF C_{mq}

The aerodynamic derivative C_{mq} is a function of the decay rate of the oscillations in the flow. However, bearing friction also contributes to decay; this effect must also be evaluated. Two separate decay tests were made, the first in the evacuated tunnel with no flow but with a quartz fiber serving as a torsion spring. The second test was the same as above (quartz spring was retained) except that the model was exposed to the airflow.

The equations of motion for these systems are:

No Flow

$$\ddot{\alpha} + d\dot{\alpha} + f\alpha = 0 \quad (A-1)$$

Flow

$$\ddot{\alpha} + b\dot{\alpha} + d\dot{\alpha} + k\alpha + f\alpha = 0 \quad (A-2)$$

$$= \ddot{\alpha} + (b+d)\dot{\alpha} + (k+f)\alpha = 0$$

where: d = effective damping coefficient
of bearings and quartz fiber

f = restoring moment coefficient
of fiber

δ = logarithmic decrement of oscillations

$$\delta \approx \frac{(\alpha_o)_n - (\alpha_o)_{n+1}}{(\alpha_o)_n}$$

and $\delta = \frac{T}{2} B$ where $B = \alpha$ coefficient in general

$$\delta = \frac{(\alpha_o)_n - (\alpha_o)_{n+1}}{(\alpha_o)_n} = \frac{T}{2} B$$

$$B = \frac{2}{(\alpha_o)_n} \frac{(\alpha_o)_n - (\alpha_o)_{n+1}}{T} = \frac{2}{(\alpha_o)_n} D$$

$$B_F = \frac{2}{(\alpha_o)_n} D_F = b + d$$

$$B_{NF} = \frac{2}{(\alpha_o)_n} D_{NF} = d$$

where the subscripts F and NF refer to the flow and no flow cases respectively

$$\text{Since } b = (b + d) - d$$

$$b = \frac{2}{(\alpha_o)_n} [D_F - D_{NF}]$$

$$\text{also } b = \frac{\rho U}{2} \frac{SL^2}{I} [-C_{mq}]$$

$$\therefore C_{mq}(\alpha_o) = - \frac{4I}{\rho U S L^2} \frac{D_F - D_{NF}}{\alpha_o} \quad (A-3)$$

at any α_o can be found by measuring the decay rates under flow and no flow conditions. This analysis assumes that bearing friction produces linear (viscous) damping. The bearing friction is most likely nearer sliding or Coulomb friction, but here this non-linearity is neglected and has been replaced by the "equivalent" viscous damping.

APPENDIX B

MOMENT OF INERTIA DETERMINATION

The mass moment of inertia (I) was found by oscillating the system in an evacuated tunnel using the quartz torsion spring and observing the period of oscillation on the counter. Two tests were made, one with the system as used in the flow tests, and a second using an additional cross arm, of known moment of inertia I' , attached to the sting. Since

$$T \sim I^{1/2}$$

then

$$\frac{T_{\text{with arm}}}{T_{\text{without arm}}} = \sqrt{\frac{I_{\text{w/arm}}}{I_{\text{w/o arm}}}}$$

or

$$\begin{aligned} I_{\text{w/o arm}} = I &= I_{\text{w/arm}} \left(\frac{T_{\text{w/o arm}}}{T_{\text{w/arm}}} \right)^2 \\ &= (I' + I) \left(\frac{T_{\text{w/o arm}}}{T_{\text{w/arm}}} \right)^2 \end{aligned}$$

$$I = \frac{I' \left(\frac{T_{\text{w/o arm}}}{T_{\text{w/arm}}} \right)^2}{I \left(\frac{T_{\text{w/o arm}}}{T_{\text{w/arm}}} \right)^2} \quad (\text{B-1})$$

This indirect method permits accurate determination of I without knowing the spring constant of the quartz spring. This test was performed with both the 9° and 45° cones, and in both cases $I' \approx 3I$.

APPENDIX C
ERROR ANALYSIS

$\frac{C}{m_{\alpha}}$

The following uncertainty values have been assigned:

$$\left(\frac{1}{2} \rho U^2 \right)^* = \pm 2.0\%$$

$$I^* = \pm 0.4\%$$

$$S^*, L^* = \pm 0.2\%$$

$$U^* = \pm 1.0\%$$

$$T^* = 1.0\%$$

$$\alpha_o^* = \pm 1\%$$

where $\left(\frac{1}{2} \rho U^2 \right)^*$, I^* , indicate uncertainty in $\left(\frac{1}{2} \rho U^2 \right)$, uncertainty in I , etc.

A least count analysis would indicate an uncertainty of $\pm 0.8\%$ in $\left(\frac{1}{2} \rho U^2 \right)^*$; however, past experience has shown that the figure of $\pm 2\%$ is more realistic due to non-uniform flow in the nozzle.

Using the 4-m-s method of error calculation,

$$\begin{aligned} C_{m_{\alpha}}^* &= \pm \sqrt{(2T^*)^2 + (I^*)^2 + \left(\frac{1}{2} \rho U^{2*} \right)^2 + (S^*)^2 + (L^*)^2} \\ &= \pm 2.9\% \end{aligned}$$

This is the error in $C_{m_{\alpha}}$ as observed. Since there is an uncertainty in the value of α_o , an additional uncertainty in $C_{m_{\alpha}}(\alpha_o)$ arises. Examples for both models will be given.

45° Cone

$C_{m\alpha}$ changes about 0.009 per degree of α_o

$$\alpha_o = 30^\circ$$

$$\frac{0.009}{0.765} = 1.2\%$$

$$C_{m\alpha}^* = \sqrt{2.9^2 + 1.2^2} = 3.1\%$$

$$\alpha_o = 15^\circ$$

$$\frac{0.009}{0.896} = 1.0\%$$

$$C_{m\alpha}^* = \sqrt{2.9^2 + 1.0^2} = 3.0\%$$

9° Cone

$C_{m\alpha}$ changes 0.008 per degree of α_o

$$\alpha_o = 20^\circ$$

$$\frac{0.008}{0.761} = 1.1\%$$

$$C_{m\alpha}^* = \sqrt{2.9^2 + 1.1^2} = 3.1\%$$

$\alpha_o = 10^\circ$ (The worst case) - $C_{m\alpha}$ changes 0.014 per degree of α_o

$$\frac{0.014}{0.666} = 2.1\%$$

$$C_{m\alpha}^* = \sqrt{2.9^2 + 2.1^2} = 3.6\%$$

$C_{m\alpha}$

The uncertainty for the 45° cone at $\alpha_o = 12.5^\circ$ will be taken for illustration.

$$D = \text{rate of decay of oscillation} = \frac{\text{amount of decay}}{\text{time to decay}}$$

$$= \frac{(\alpha_o)_1 - (\alpha_o)_2}{t_2 - t_1} = \frac{15^\circ - 10^\circ}{t_{10} - t_{15}}$$

The scatter of data indicates that the average time figures are accurate within $\pm 2\%$, and using $\alpha_o^* = \pm 1^\circ$

$$\left\{ \begin{array}{l} (\alpha_o)_1 - (\alpha_o)_2 = 15 - 10 = 5^\circ \\ [(\alpha_o)_1 - (\alpha_o)_2]^* = \sqrt{1^2 + 1^2} = 1.4 = 28\% \end{array} \right.$$

$$\left\{ \begin{array}{l} t_2 - t_1 = 160 - 107 = 53 \quad \text{Flow Test} \\ [t_2 - t_1]^* = \sqrt{3.2^2 + 2.2^2} = 3.2 = 7.1\% \end{array} \right.$$

$$\left\{ \begin{array}{l} t_2 - t_1 = 157 - 109 = 48 \quad \text{No Flow Test} \\ t_2 - t_1^* = \sqrt{3.1^2 + 2.2^2} = 3.8 = 8.0\% \end{array} \right.$$

$$D^* = \sqrt{[(\alpha_o)_1 - (\alpha_o)_2]^*^2 + [t_2 - t_1]^*^2}$$

$$D_F^* = \sqrt{28^2 + 7.1^2} = 29\%$$

$$D_{NF}^* = \sqrt{28^2 + 8.1^2} = 29\%$$

$$D_F - D_{NF} = 0.09434 - 0.1042 = -0.0099$$

$$[D_F - D_{NF}]^* = \sqrt{0.027^2 + 0.030^2} = 0.041 = 41\%$$

\bar{C}_{mq} is a direct function of $D_F - D_{NF}$ and therefore \bar{C}_{mq} will have

an uncertainty of at least 410%. All other values of \bar{C}_{mq} show a similarly large uncertainty, this example being typical.

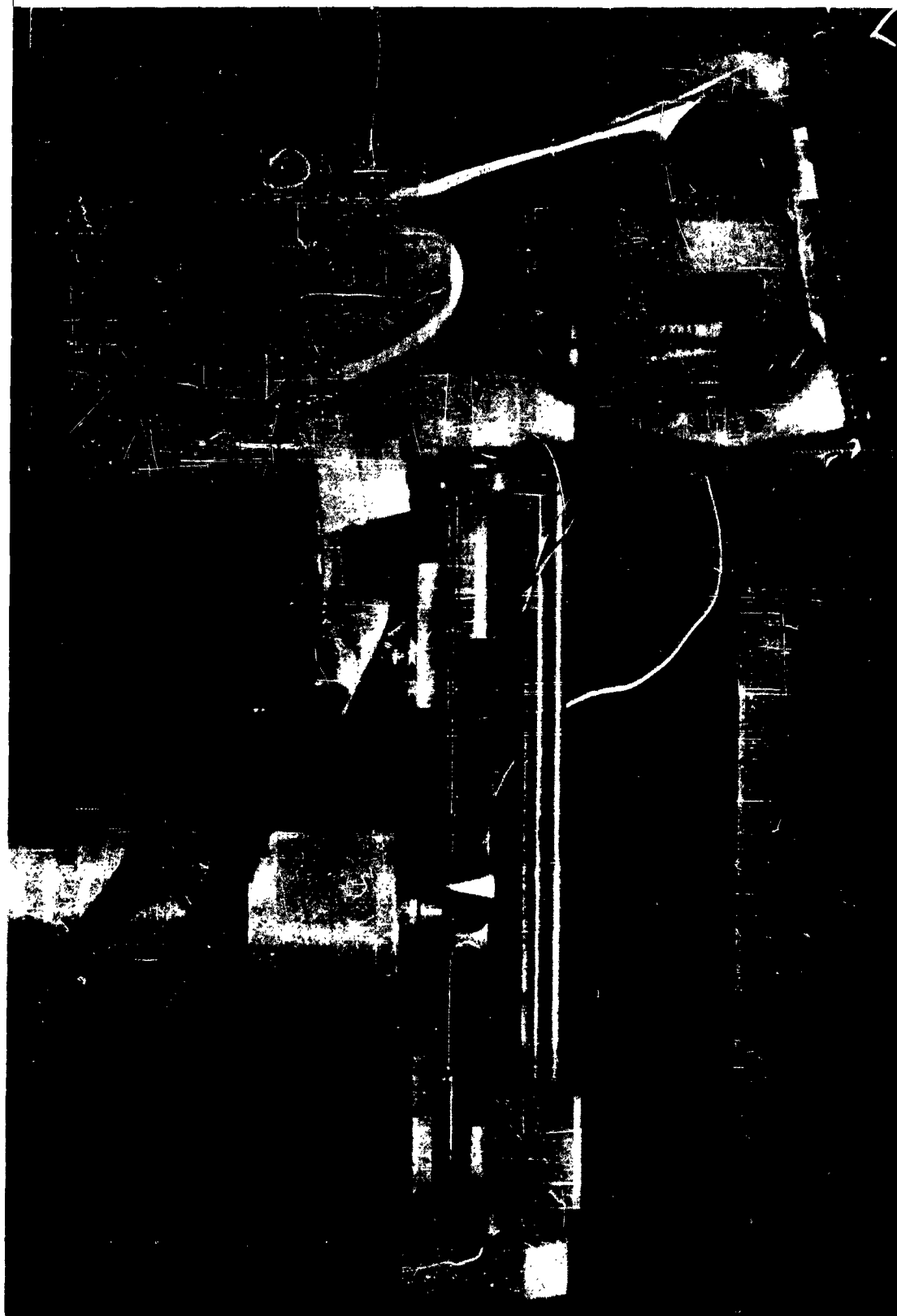


FIG.1 FIXTURE MOUNTED ON NOZZLE WITH 45° CONE

HYD 7610

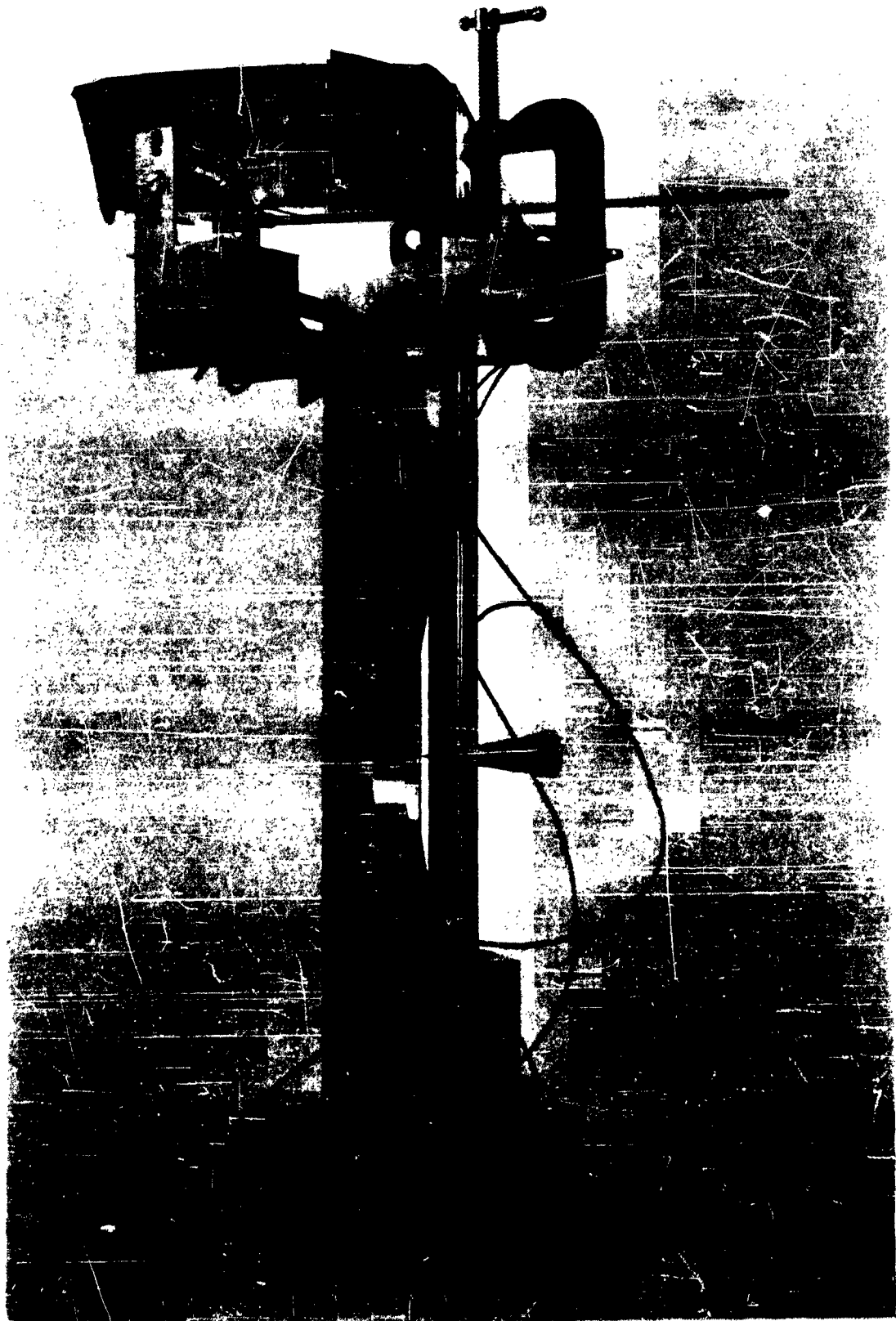


FIG. 2 FIXTURE WITH 9° CONE

HYD 7611

α_0	$\bar{C}_{m\alpha}$ 45° CONE	$\bar{C}_{m\alpha}$ 9° CONE
3°	1.007	0.582
5°	0.994	0.598
10°	0.949	0.666
15°	0.896	0.722
20°	0.851	0.762
30°	0.765	0.803

FIG. 3 VALUES OF $\bar{C}_{m\alpha}$ FOR VARIOUS
OSCILLATION ANGLES (α_0) .
45° & 9° SEMI- VERTEX ANGLE
CONES.

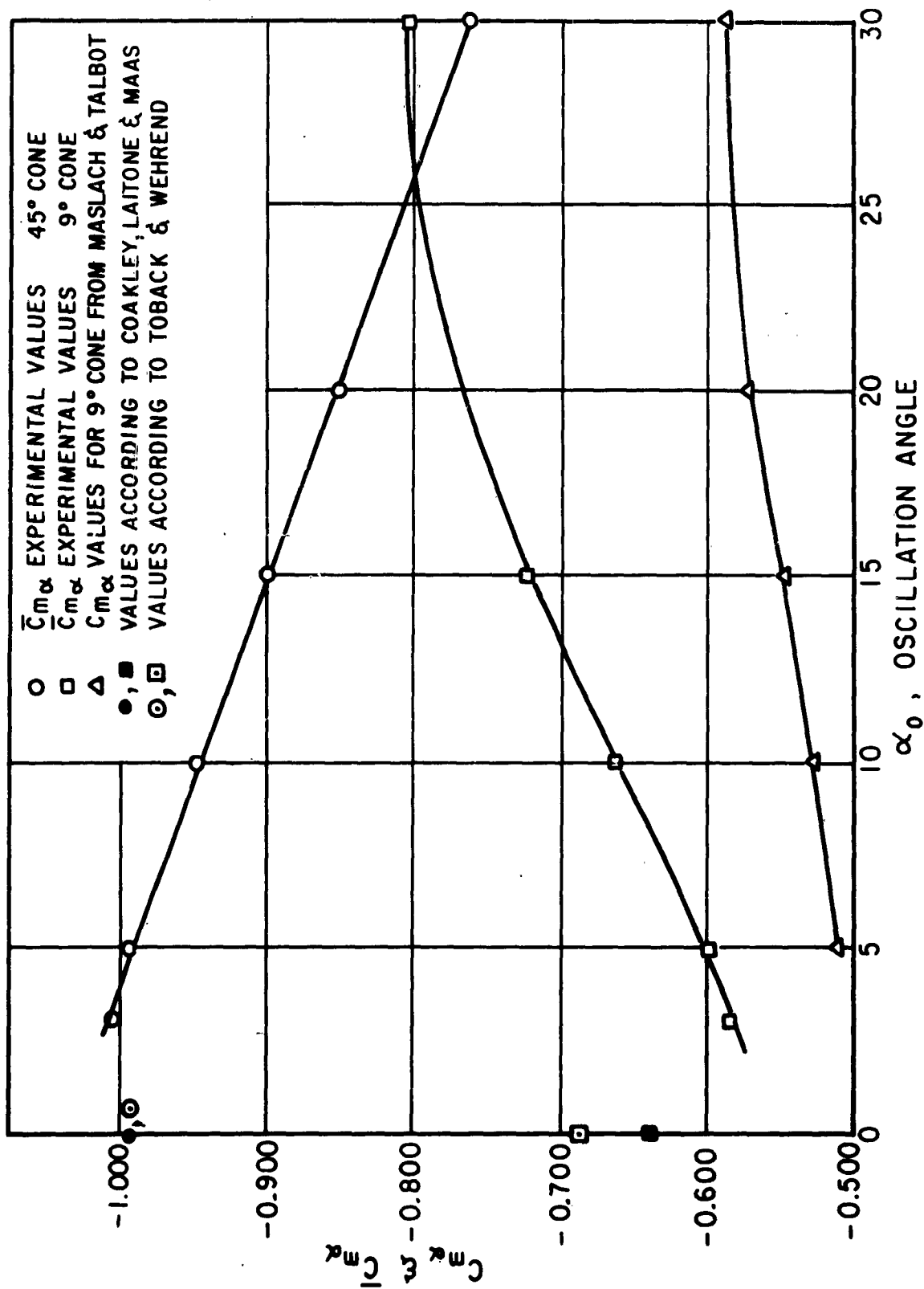
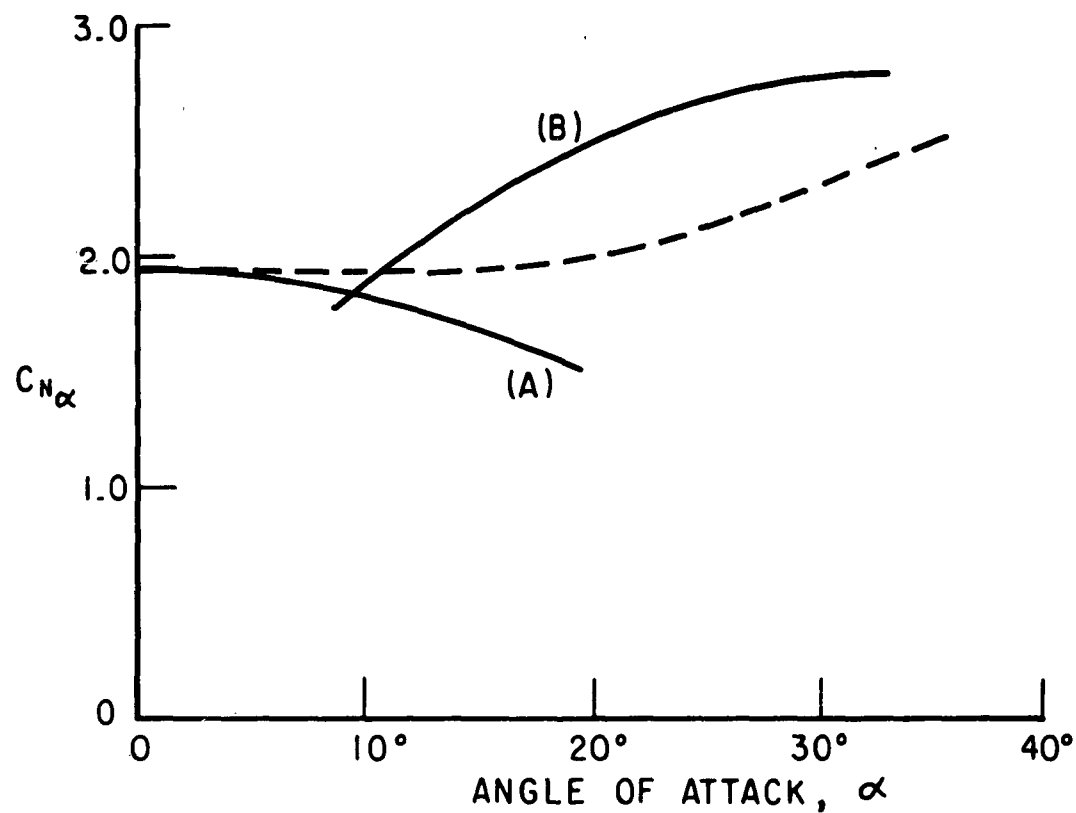


FIG. 4 $\bar{C}_{m\alpha}$ & $C_{m\alpha}$ AS A FUNCTION OF OSCILLATION ANGLE



(A) SOLUTIONS FOR $\alpha < \gamma$

(B) SOLUTIONS FOR ONE HALF OF THE SURFACE SEEING THE FLOW.

FIG. 5 $C_{N\alpha}$ vs α
NEWTONIAN FLOW SOLUTION

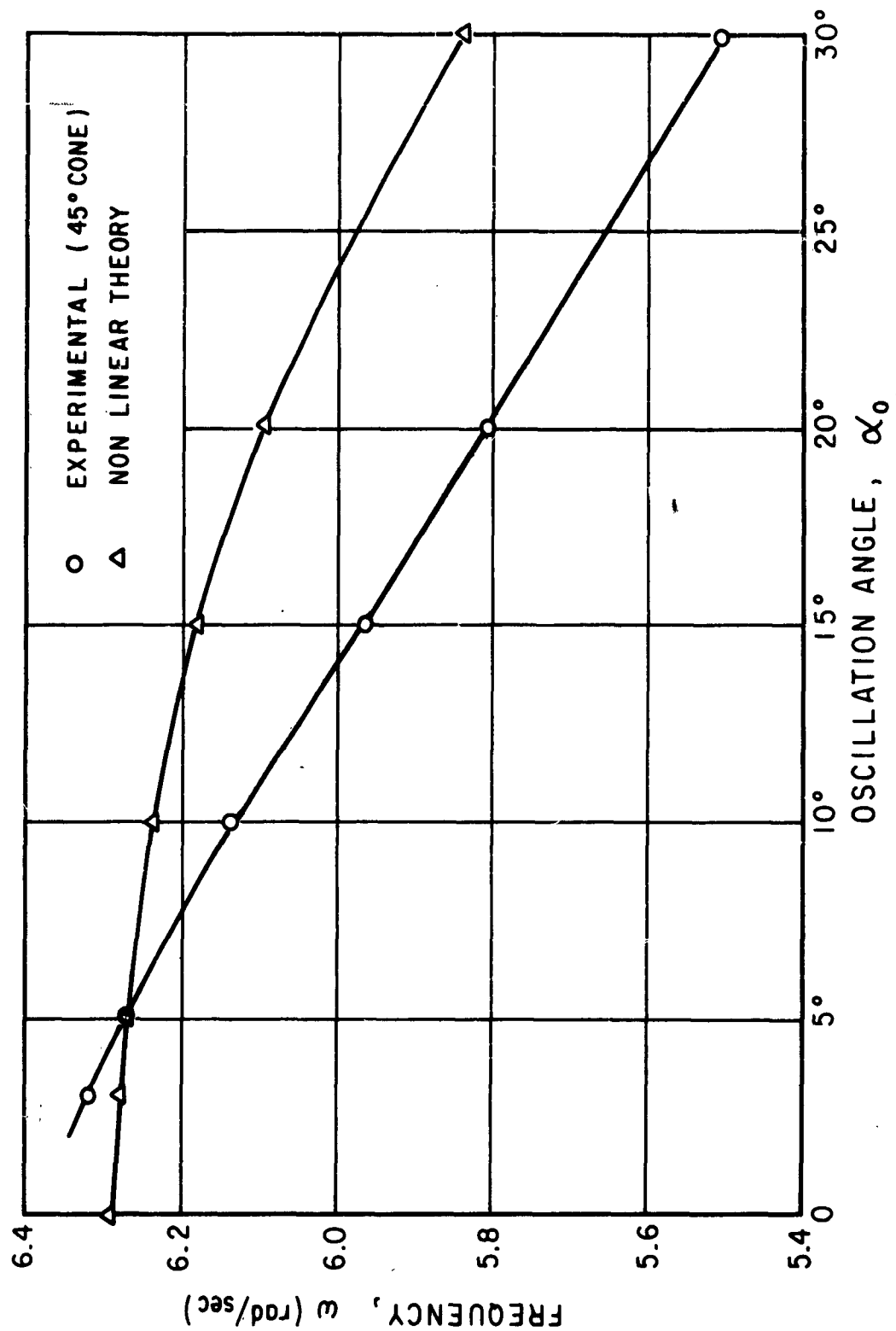


FIG. 6 OSCILLATION FREQUENCY vs ANGLE

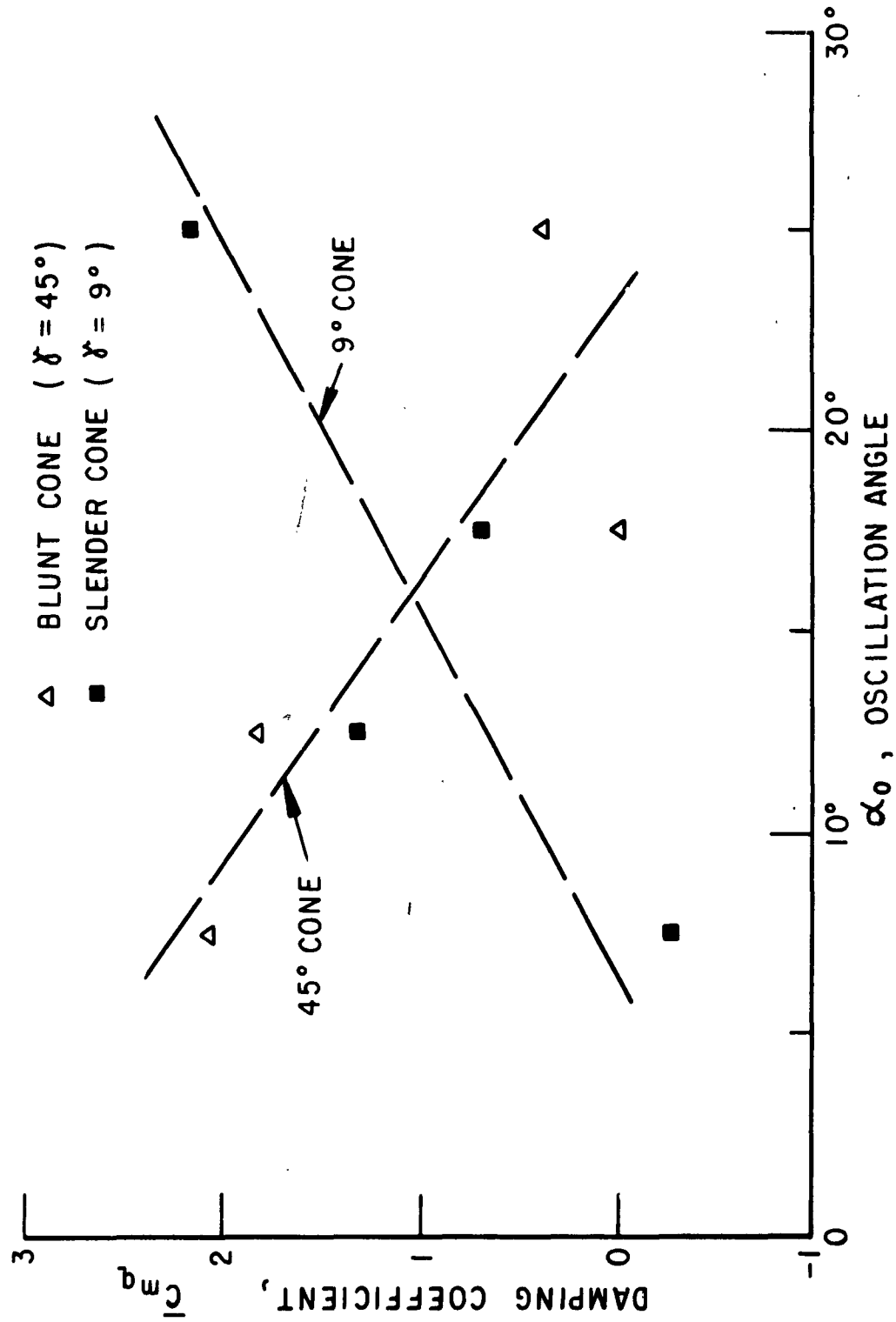


FIG. 7 PLOT OF \bar{C}_{mq} vs OSCILLATION ANGLE

AUTOMATIC DISTRIBUTION LIST FOR UNCLASSIFIED
TECHNICAL REPORTS - 9-18-59

NAVY

Chief of Naval Research Department of the Navy Washington 25, D. C. Attn: Code 438 (2) Code 419 (1) Code 461 (1)	Chief, Bureau of Aeronautics Department of the Navy Washington 25, D. C. Attn: Research Division Aero & Hydro Branch (2)
Commanding Officer Office of Naval Research Branch Office 150 Causeway Street Boston, Massachusetts (1)	Commanding Officer and Director David Taylor Model Basin Carderock, Maryland Attn: Aerodynamics Laboratory (1)
Commanding Officer Office of Naval Research Branch Office The John Crerar Library Building 86 East Randolph Street Chicago 1, Illinois (1)	Chief, Bureau of Ordnance Department of the Navy Washington 25, D. C. Attn: Code Re 0 (1) Code Re S1-e (1)
Commanding Officer Office of Naval Research Branch Office 346 Broadway New York 13, New York (1)	Commander Dahlgren Proving Ground Dahlgren, Virginia Attn: Technical Library (1)
Commanding Officer Office of Naval Research Branch Office 1030 East Green Street Pasadena 1, California (1)	Commander Naval Ordnance Test Station Inyokern, China Lake, California Attn: Technical Library (1) Code 501 (1)
Commanding Officer Office of Naval Research Fleet Post Office Navy No. 100, Box 39 New York, New York (15)	Commander Naval Ordnance Laboratory White Oak, Maryland Attn: Hyperballistics Division (1) Aeroballistics Division (1) Aerophysics Division (1)
Commanding Officer Office of Naval Research Branch Office 1000 Geary Boulevard San Francisco 9, California (2)	Commander Office of Scientific Research Air Research & Development Command P.O. Box 1395 Baltimore 3, Maryland (1)
Director Naval Research Laboratory Washington 25, D. C. Attn: Code 2021 (6)	Chief, Bureau of Yards & Docks Department of the Navy Washington 25, D. C. Attn: Plans & Research Section (1)
	Superintendent Naval Postgraduate School Monterey, California (1)

NAVY (cont'd)

U.S. Naval Air Material Test Center
Point Mugu, California
Attn: Chief Scientist (1)

AIR FORCE

Commander
AF Office of Scientific Research
Washington 25, D. C.
Attn: Mechanics Division (1)

Director
Office for Advanced Studies
AF Office of Scientific Research
Box 2035
Pasadena 2, California (1)

Commander
Western Development Division
Air Research & Development Command
P. O. Box 262
Inglewood, California (1)

Commander
Air Force Cambridge Research Center
230 Albany Street
Cambridge 39, Massachusetts
Attn: Geo-Phys. Research Library (1)

Commander
AF Missile Test Center
(AFMTC Tech Library MU-135)
Patrick AFB, Florida (1)

Arnold Engineering Development
Center Library
P. O. Box 162
Tullahoma, Tennessee
Attn: Dr. J. Lukasiewicz (2)

Commander
Wright Air Development Center
Wright-Patterson Air Force Base
Dayton, Ohio
Attn: Aeronautical Research Lab (1)
Aircraft Laboratory (1)

ARMY

Office of Ordnance Research
Department of the Army
Duke Station
Durham, North Carolina (1)

Ballistics Research Laboratory
Aberdeen Proving Ground
Aberdeen, Maryland
Attn: Dr. R. H. Kent (1)
Dr. F. D. Bennett (1)

Internal Ballistics Laboratory
Aberdeen Proving Ground
Aberdeen, Maryland
Attn: Dr. J. H. Frazer (1)

Commanding General
Redstone Arsenal, U.S. Army
Redstone Arsenal, Alabama
Attn: Technical Library (1)

NASA

Director of Research
National Aeronautics and Space
Administration
1512 H Street, N.W.
Washington 25, D. C. (5)

Director
Langley Research Center, NASA
Langley Field
Hampton, Virginia (1)

Director
Ames Research Center, NASA
Moffett Field, California (1)

Director
Lewis Research Center, NASA
21000 Brookpark Road
Cleveland 35, Ohio (1)

Western Coordination Office
National Aeronautics and Space
Administration
7660 Beverly Boulevard
Los Angeles, California (1)

DEPARTMENT OF DEFENSE

Chief
Armed Forces Special Weapons Project
P. O. Box 2610
Washington 25, D. C. (1)

Executive Secretary
Weapons System Evaluation Group
Office of Secretary of Defense
The Pentagon
Washington 25, D. C. (1)

OTHER GOVERNMENT AGENCIES

Director
National Bureau of Standards
Washington 25, D. C.
Attn: Fluid Mechanics Section (1)
Electron Physics Section (1)

U.S. Atomic Energy Commission
Technical Information Service
Washington 25, D. C.
Attn: Technical Librarian (1)

National Science Foundation
Division of Mathematical, Physical
and Engineering Sciences
Washington 25, D. C. (1)

Documents Service Center
Armed Services Technical
Information Agency
Arlington Hall Station
Arlington 12, Virginia (10)

Office of Technical Services
Department of Commerce
Washington 25, D. C. (1)

EDUCATIONAL INSTITUTIONS

Prof. R. F. Probstain
Division of Engineering
Brown University
Providence 12, Rhode Island (1)

Aeronautical Laboratory
Division of Engineering
Brown University
Providence 12, Rhode Island
Attn: Dr. Maeder (1)

Metcalf Laboratory
Brown University
Providence 12, Rhode Island
Attn: Prof. D. F. Hornig (1)

Los Alamos Scientific Laboratory
University of California
Los Alamos, New Mexico
Attn: Theoretical Division, (1)
Dr. J. L. Tuck (1)
Dr. R. G. Shreffler (1)
J-1 Division, (1)
Drs. Duff and Graves (1)

Jet Propulsion Laboratory
California Institute of Technology
Pasadena 4, California
Attn: Dr. P. Wegener (1)

Guggenheim Aeronautical Laboratory
California Institute of Technology
Pasadena 4, California
Attn: Prof. C.B. Millikan, Director (1)
Prof. Lester Lees (1)
Prof. H. W. Liepmann (1)
Prof. J. Cole (1)

Department of Physics
California Institute of Technology
Pasadena 4, California
Attn: Prof. F. Zwicky (1)

Radiation Laboratory
University of California
Livermore, California
Attn: Dr. S. A. Colgate (1)
Dr. R. Post (1)

Department of Aerodynamics
Case Institute of Technology
Cleveland 6, Ohio
Attn: Prof. G. Kuerti (1)

Yerkes Observatory
University of Chicago
Williams Bay, Wisconsin
Attn: Prof. S. Chandrasekhar (1)

Graduate School of Aeronautical
Engineering
Cornell University
Ithaca, New York
Attn: Prof. W. Sears (1)
Prof. E. L. Resler, Jr. (1)

EDUCATIONAL INSTITUTIONS - (Cont'd)

Cornell Aeronautical Laboratory
4455 Genessee Street
Buffalo, New York
Attn: Dr. A. Hertzberg (1)

Department of Engineering Sciences
Harvard University
Cambridge 38, Massachusetts
Attn: Prof. G. Carrier (1)
Prof. H. Emmons (1)

Harvard Observatory
Harvard University
Cambridge, Massachusetts
Attn: Prof. F. Whipple (1)

Dr. H. Kendall Reynolds
Physics Department
The University of Houston
3801 Cullen Boulevard
Houston 4, Texas (1)

Department of Aeronautical Engineering
University of Illinois
Urbana, Illinois
Attn: Prof. H. S. Stillwell,
Chairman (1)

Armour Research Foundation
Illinois Institute of Technology
Chicago 16, Illinois (1)

Applied Physics Laboratory
Johns Hopkins University
P.O. Box 244 - Rt. 1
Laurel, Maryland
Attn: Dr. F. N. Frenkiel
Technical Reports Office (2)

Department of Physics
Lehigh University
Bethlehem, Pennsylvania
Attn: Prof. R. J. Emrich (1)

Institute for Fluid Mechanics
and Applied Mathematics
University of Maryland
College Park, Maryland
Attn: Prof. Burgers (1)

Department of Aeronautics
Johns Hopkins University
Baltimore 18, Maryland
Attn: Prof. F. H. Clauser (1)

Department of Aeronautical Engineering
Massachusetts Institute of Technology
Cambridge 39, Massachusetts
Attn: Prof. H. G. Stever (1)
Prof. L. Trilling (1)

Department of Mathematics
Massachusetts Institute of Technology
Cambridge 39, Massachusetts
Attn: Prof. C. C. Lin (1)

Department of Mechanical Engineering
Massachusetts Institute of Technology
Cambridge 39, Massachusetts
Attn: Prof. J. Kaye (1)

Department of Aeronautical Engineering
University of Michigan
Ann Arbor, Michigan
Attn: Prof. O. Laporte (1)
Prof. G. Uhlenbeck (1)

Department of Astronomy
University of Michigan
Ann Arbor, Michigan
Attn: Prof. L. Goldberg (1)

Department of Aeronautical Engineering
University of Minnesota
Minneapolis, Minnesota
Attn: Prof. J.D. Akerman, Chairman (1)

Institute of Meteoritics
University of New Mexico
Albuquerque, New Mexico
Attn: Prof. L. LaPaz (1)

Institute for Mathematics and Mechanics
New York University
25 Waverly Place
New York 3, New York
Attn: Prof. R. Courant, Director (1)
Prof. J. Stoker (1)

Guggenheim School of Aeronautics
New York University
New York 53, New York
Attn: Prof. J.F. Ludloff (1)

Department of Mechanical Engineering
Northwestern University
Evanston, Illinois
Attn: Prof. A. R. Cambel (1)

EDUCATIONAL INSTITUTIONS - (Cont'd)

Department of Physics
University of Oklahoma
Norman, Oklahoma
Attn: R.G.Fowler (1)

Dr. Loren E. Bollinger
The Ohio State University
Rocket Research Laboratory
2240 Olentangy River Road
Columbus 10, Ohio (1)

Aerodynamics Laboratory
Polytechnic Institute of Brooklyn
Freeport, L.I., New York
Attn: Prof. A. Ferri (1)

Palmer Physical Laboratory
Princeton University
Princeton, New Jersey
Attn: Prof. W. Bleakney (1)
Prof. W.C.Griffith (1)

Princeton University
The James Forrestal Research Center
Princeton, New Jersey
Attn: Prof.S.M.Bogdonoff, Bldg.D (1)

Princeton University
The James Forrestal Research Center
Princeton, New Jersey
Attn: Prof.W.D.Hayes, Sayre Hall (1)

Princeton University Observatory
Princeton, New Jersey
Attn: Prof. L. Spitzer, Jr. (1)

Department of Aeronautical Engineering
Rensselaer Polytechnic Institute
Troy, New York
Attn: Profs. Harrington & Foa (1)

Engineering Center
University of Southern California
University Park
Los Angeles 7, California
Attn: Drs.R.Chuan & C.L.Daily (1)

Guggenheim Aeronautical Laboratory
Stanford University
Standord, California
Attn: Prof. W. Vincenti (1)

Defense Research Laboratory
University of Texas
P. O. Box 8029
Austin, Texas
Attn: M.J.Thompson (1)

College of Engineering
University of California, Los Angeles
Los Angeles 24, California
Attn: Dean L.M.K. Boelter (1)

Department of Physics
University of California, Los Angeles
Los Angeles 24, California
Attn: Prof. J. Kaplan (1)

Experimental Research Group
University of Utah
Salt Lake City, Utah
Attn: Prof. M.A.Cook, Director (1)

Department of Aeronautical Engineering
University of Washington
Seattle 5, Washington
Attn: Department Librarian (1)

Department of Chemistry
University of Wisconsin
Madison, Wisconsin
Attn: Prof. J.O.Hirschfelder (1)

Sterling Chemistry Laboratory
Yale University
New Haven, Connecticut
Attn: Prof. J.G.Kirkwood (1)

CANADA

Institute of Aerophysics
University of Toronto
Toronto 5, Canada
Attn: Dr.G.N.Patterson, Director (1)

Division of Mechanical Engineering
National Research Laboratories
Ottawa, Canada
Attn: Dr: K. Orlik, Dr. Ruckemann (1)

United Aircraft Corporation
Research Department
362 Main Street
East Hartford 8, Connecticut (1)

INDUSTRIAL ORGANIZATIONS

Aerojet Engineering Corporation 6352 North Irwindale Avenue Box 296 Azusa, California	(1)	Fairchild Engine & Aircraft Company Fairchild Engine Division Farmingdale, L.I., New York Attn: Mrs. C. Minck, Librarian	(1)
ARO, Inc. Tullahoma, Tennessee Attn: Drs. R.W. Perry & R. Smelt	(1)	Flight Sciences Laboratory, Inc. 1965 Sheridan Drive Buffalo 23, New York Attn: Dr. J. S. Isenberg, Technical Director	(1)
Miss Spence, Librarian AVCO Manufacturing Company Research Laboratories 2385 Revere Beach Parkway Everett 49, Massachusetts Attn: Drs. Kantrowitz & Lin	(2)	General Applied Science Laboratories Meadowbrook National Bank Building 60 Hempstead Avenue Hempstead, New York Attn: Jane L. Herod, Librarian	(1)
AVCO Manufacturing Company Lycoming Division Stratford, Connecticut Attn: Dr. J. C. Keck	(1)	General Electric Company Research Laboratory P. O. Box 1088 Schenectady, New York Attn: Drs. Nagamatsu, White, and Alpher	(1)
Boeing Airplane Company Box 3107 Seattle 14, Washington	(1)	General Electric Company Special Defense Projects Department 3198 Chestnut Street Philadelphia 4, Pennsylvania Attn: Aerophysics Lab. Operation Dr. J. Farber	(2)
Borg-Warner Corporation Research Center Applied Physics Group Des Plaines, Illinois	(1)	Dr. Gottfried K. Wehner Mechanical Division General Mills, Inc. 1620 Central Avenue Minneapolis 13, Minnesota	(1)
Chance-Vought Aircraft Corporation Dallas, Texas	(1)	The Glenn L. Martin Company Department 520, Mail No. 3072 Baltimore 3, Maryland Attn: Mr. L. Cooper	(1)
CONVAIR San Diego Division San Diego 12, California Attn: Dr. W. H. Dorrance	(1)	Grumman Aircraft Engineering Corp. Bethpage, L.I., New York	(1)
Air Force Plant Representative San Antonio Air Material Area CONVAIR-Astronautics San Diego 12, California	(1)	Hughes Aircraft Corporation Research and Development Laboratory Culver City, California Attn: Dr. A. E. Puckett	(1)
Douglas Aircraft Company, Inc. 3000 Ocean Park Boulevard Santa Monica, California	(1)	Hydronautics, Incorporated 200 Monroe Street Rockville, Maryland Attn: Mr. Phillip Eisenberg Mr. Marshall P. Tulin	(1)
Fairchild Engine & Aircraft Company Guided Missiles Division Wyandanch, L.I., New York	(1)		

INDUSTRIAL ORGANIZATIONS - (Cont'd)

Technical Information Center, 50-21
Lockheed Missiles and Space Division
P. O. Box 504
Sunnyvale, California (1)

Marquardt Aircraft Corporation
7801 Havehurst
Van Nuys, California (1)

Midwest Research Institute
Department of Physics
4049 Pennsylvania Avenue
Kansas City, Missouri
Attn: Mr. K.L. Sandefur (1)

North American Aviation, Inc.
Aerophysics Department
12214 Lakewood Boulevard
Downey, California
Attn: Dr. van Driest (1)

Northrop Aircraft, Inc.
Northrop Field
Hawthorne, California (1)

Technical Librarian
Ramo-Wooldridge Corporation
8820 Bellanca Avenue
Los Angeles 45, California
Attn: Drs. M.U. Clauser, Doll,
& J. Logan (2)

RAND Corporation
1700 Main Street
Santa Monica, California
Attn: E.P. Williams &
C. Gasley, Jr. (1)

Republic Aviation Corporation
Farmingdale, L.I., New York (1)

Sandia Corporation
Sandia Base
Albuquerque, New Mexico
Attn: Drs. C.C. Hudson, M.L. Merritt,
& J.D. Shreve, Jr. (1)

Stanford Research Institute
Poulter Laboratories
Palo Alto, California
Attn: Drs. Poulter & Duvall (1)

Therm Advanced Research
Therm, Incorporated
Ithaca, New York
Attn: Dr. A. Ritter (1)

SPECIAL ADDITIONAL LIST FOR
THEORETICAL PAPERS

Professor M. Holt
Division of Applied Mathematics
Brown University
Providence 12, Rhode Island (1)

Professor H. Lewy
Applied Mathematics Group
Mathematics Department
University of California
Berkeley 4, California (1)

Professor D. Gilbarg
Graduate School for Applied Mathematics
Indiana University
Bloomington, Indiana (1)

Librarian
Graduate School for Applied Mathematics
Indiana University
Bloomington, Indiana (1)

Dr. G. Griderley
P. O. Box 186
Fairborn 4, Ohio (1)

SPECIAL ADDITIONAL LIST FOR
RAREFIED GASES

Mr. K. M. Siegel
Upper Atmosphere Section
Willow Run Research Center
University of Michigan
Ypsilanti, Michigan (1)

Professor A. H. Kuhlthau
Department of Physics
University of Virginia
Charlottesville, Virginia (1)

Australian Weapons Research Establishment
c/o Defence Res. & Dev. Representative
Australian Joint Service Staff
P.O. Box 4837
Washington 8, D. C. (1)